Implementation and Verification of NorSand Model in General 3D Framework

Zhao Cheng, Ph.D., P.E., M.ASCE[1]; and Michael Jefferies, P.Eng.[2]

[1]Itasca Consulting Group, Inc., Minneapolis, MN. E-mail: zcheng@itascacg.com
[2]Consulting Engineer, Lincoln, U.K. E-mail: geomek@hotmail.com

ABSTRACT

NorSand is a critical state (plasticity) model for soils in which particle to particle interactions are controlled by contact forces and slips. The state parameter allows capturing soil behavior over a wide range of confining stresses and densities using relatively few and familiar soil properties that can be determined from the routine laboratory or in situ tests. This paper presents the implementation of NorSand in the leading geotechnical software platform FLAC3D. This implemented version includes the usual three-dimensional aspects allowing for the proportion of intermediate principal stress as well as the far less common feature of principal stress rotation; these aspects allow simulation of cyclic mobility as well as static liquefaction. The results are cross-verified with a VBA-coded spreadsheet for simulations of various densities, drainage conditions, and test types, including triaxial compression and simple shear.

INTRODUCTION

Many geotechnical failures cannot be predicted by simple constitutive models for soils, including the typical brittle strength-loss (static liquefaction) of a loose soil structure being over-surcharged, slope-steepened, or subject to rising pore pressure. The importance of modern computational soil mechanics has become evident in the past few years where only this approach was able to show how and why two very large dam failures developed, i.e., the failures of Fundao (Morgenstern et al. 2016) and Cadia (Morgenstern et al. 2019). But this presents a challenge for geotechnical engineers, as commercial software has lagged in offering appropriate constitutive models for liquefaction (however it is caused); the cited failure investigations adopted a user-defined model that involved specialist skills rarely found in geotechnical practice. Clearly, much can be gained by making these modern approaches to soil behavior more accessible to geotechnical practice.

Critical State Soil Mechanics (CSSM) originated in a response of the Corps of Engineers to avoid rather frequent failures of hydraulic fill dams pre-1920. CSSM fits within the theory of work hardening plasticity, a thread on soil behavior developing over some 100 years with contributions from many workers. CSSM has become essentially a mature understanding; Jefferies and Been (2016) provide a history of the stages in the development of CSSM. CSSM offers: 1) a natural response to the effect of changes in confining stress and void ratio on soil behavior through the state parameter; and 2) soil properties that are both familiar and unaffected by stress level or soil density. There are several “flavors” of CSSM; the variant used here is the NorSand model, which is a strict implementation of Drucker et al. (1957). The original “fundamental” derivations are found in Jefferies (1993) with the generalization in Jefferies and Shuttle (2002). Despite its name, NorSand can be used for all soils as particle to particle interactions that are controlled by contact forces and slips rather than bonds. The theory has no concept of “geology”; NorSand was used to represent loose silt liquefaction for both Fundao and Cadia analyses.

FLAC is an explicit finite-difference program widely used in geotechnical engineering and

was adopted for the analysis of the Fundao and Cadia failures. NorSand was used as a user-defined model in these analyses, which is less than optimal in terms of speed and convenience. The upcoming release of *FLAC* (Itasca 2019a) version 8.1 and *FLAC3D* (Itasca 2019b) version 7.0 now include NorSand as a built-in soil model. Full benefits of *FLAC*, including fluid-mechanical coupling and large-strain mode with updating of the grid applies to the implemented NorSand model. Here we describe the implementation of NorSand in *FLAC3D*, including features such as principal stress rotation. Verifications and illustration examples are presented.

FORMULATIONS

Both stress and strain are assumed positive in tension and negative for compression following the convention of the software platform. Pressures (e.g., mean pressure, pore pressure) are assumed positive in compression. If not explicitly stated otherwise, the stresses and material properties are "effective" by default. The superscripts e and p denote the elastic and plastic parts, respectively.

Elasticity: In this implementation version, the elasticity assumes the elastic shear G and bulk modulus K are

$$G = G_{ref}\left(\frac{p}{p_{ref}}\right)^{m},\ K = \frac{2(1+\nu)}{3(1-2\nu)}G \tag{1}$$

respectively, where p is the current mean pressure, p_{ref} is a reference pressure (usually and by default, 100 kPa), G_{ref} is the reference shear modulus at the reference pressure, m is a material constant with a physical range of $0 \le m \le 1$, and ν is the Poisson's ratio, which is considered a material constant. For $m = 0$, $G = G_{ref}$, which corresponds to a constant elastic shear modulus. For $m = 1$, $G = \left(G_{ref} / p_{ref}\right) p = I_r p$, which corresponds to an elastic shear modulus being linear to the current p with a constant shear rigidity $I_p = G_{ref} / p_{ref}$.

Critical State and Image State: The critical state requires $D^p = 0$ and $\dot{D}^p / \dot{e}_q^p = 0$, where the dilatancy D^p is defined as $D^p = \dot{e}_v^p / \dot{e}_q^p$ with $\dot{e}_v^p$ and $\dot{e}_q^p$ being the rate of the plastic volumetric and deviatoric strain, respectively. If only $D^p = 0$, then this is an image state (denoted by the subscript i), variously also referred to as the pseudo steady state or phase change condition. The critical state locus (CSL) can be the traditional one defined by a two-parameter semi-logarithmic form:

$$e_c(p) = \Gamma - \lambda ln(p) \tag{2}$$

where Γ and λ are material constants, with p being the mean effective stress. However, many soils are not well represented by Equation (2) and a power-law form is popular in such instances:

$$e_c(p) = C_a - C_b\left(\frac{p}{p_{ref}}\right)^{C_c} \tag{3}$$

where C_a, C_b, and C_c are now the material constants defining the CSL.

State Parameter: The state parameter (Been and Jefferies 1985) is defined as the difference of the current void ratio, e, and the void ratio at the critical state, e_c, calculated by Equation (2) or (3) at the current pressure p:

$$\psi = e - e_c(p) \tag{4}$$

Yield Surface: The outer yield surface (Figure 1) of the NorSand model has the familiar bullet-like shape of the original Cam-Clay model, which is expressed by

$$\frac{\eta}{M_i} = 1 - ln\left(\frac{p}{p_i}\right) \tag{5}$$

where p_i is called the image stress and controls the size of the yield surface; $\eta = q/p$, $q = \sqrt{3J_2}$ and J_2 is the second invariant of the deviatoric stress tensor; M_i is defined as

$$M_i = M\left(1 - \frac{N\chi_i|\psi_i|}{M_{tc}}\right) \tag{6}$$

and M_{tc} is a material constant representing the value of η at the critical state in triaxial compression (hence subscript "tc"); $\psi_i = e - e_c(p_i)$; N is Nova's (1982) volumetric coupling coefficient; and χ_i can be approximated (Jefferies and Been 2016) by $\chi_i = M_{tc}\chi_{tc}/(M_{tc} - \lambda\chi_{tc})$ with χ_{tc} a material constant that captures state-dilatancy. M is the critical friction ratio considering the effect of the Lode's angle θ, which is simply expressed (Jefferies and Shuttle 2011) as

$$M = M(\theta) = M_{tc}g(\theta) = M_{tc}\left[1 - \frac{M_{tc}}{3 + M_{tc}}cos\left(\frac{3\theta}{2} + \frac{\pi}{4}\right)\right] \tag{7}$$

so that $M(\theta) = M_{tc}$ for $\theta = \pi/6$ at the TC condition and $M(\theta) = 3M_{tc}/(3 + M_{tc})$ for $\theta = -\pi/6$ at the TE (triaxial extension) condition.

Hardening Rule: The image stress p_i controls the size of the yield surface by the hardening rule

$$\frac{\dot{p}_i}{p_i} = H\frac{M_i}{M_{i,tc}}\left(\frac{p}{p_i}\right)^2\left(\frac{p_{i.max}}{p} - \frac{p_i}{p}\right)\dot{\varepsilon}_q^p + ST_S + T_{PSR} \tag{8}$$

where the hardening modulus is defined by $H = H_0 - H_y\psi$ with H_0 and H_y being material constants. The hardening limit $p_{i,max}$ is defined as $p_{i,max} = pexp(-\chi_i\psi_i/M_{i,tc})$, which corresponds to η_L (see Figure 1) and defines an inner surface.

The additional cap softening term T_S in Equation (8) is optional (by setting $0 \le S \le 1$). T_S is found necessary to deal with rapidly changing mean effective stress during undrained tests (Jefferies and Been 2016). In this implemented version, T_S is

$$T_S = \frac{\left(\frac{K}{p}\right)\left(\frac{\eta}{\eta_L}\right)\dot{\varepsilon}_v^p}{\left(1 + \frac{\chi_i\lambda}{M_{i,tc}}\right)} \tag{9}$$

The last term, T_{PSR} (Jefferies et al. 2015), in Equation (8) captures the effects of principal stress rotation (PSR):

$$T_{PSR} = \left[-Z\left(\frac{p_i}{p} - \frac{1}{r} \right) \left| \frac{\dot{\alpha}}{\pi} \right| + \frac{1}{r} \right] |\psi_i| \tag{10}$$

where Z is a material constant, $r = \exp(1)$ is the yield surface spacing ratio, and α is the current included angle between the direction of major principal stress and *z*-coordinate frame of reference in the 3D version. To capture the cyclic mobility in a dynamic simulation, Z should be input as a positive value.

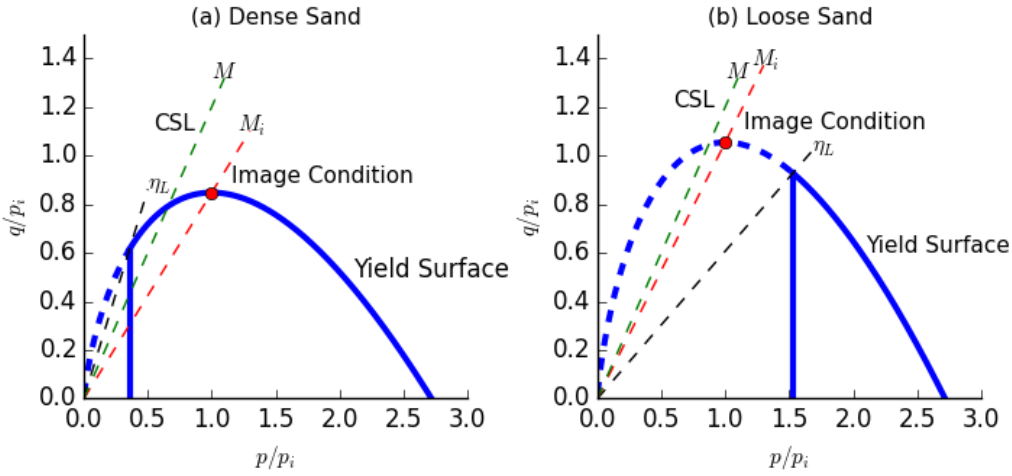

Figure 1: Illustration of NorSand yield surfaces and image stress.

IMPLMENTATION

FLAC3D uses the *elastic predictor – plastic corrector* (EP-PC) method for plasticity. The strain increment is additively decomposed into elastic and plastic parts with both plastic and elastic principal strain increments assumed coaxial with the current principal stress. The associated flow rule is adopted for plastic evolution. By rearranging the yield function in Equation (5) into $F = q - Mp + M_i p \ln(p / p_i) = 0$, we have

$$\dot{q} = 3G\left(\dot{e}_q - \dot{e}_q^p\right) = 3G\left(\dot{e}_q - \lambda^s\right), \dot{p} = K\left(\dot{e}_v - \dot{e}_v^p\right) = K\left(\dot{e}_v - \lambda^s D^p\right) \tag{11}$$

where λ^s is the plastic multiplier, which will be determined from the consistency condition. Note that in Equation (11), $\partial F / \partial q = 1$, $\partial F / \partial p = D^p = M_i - \eta$, and the associated plastic flow rule ($\dot{e}_{ij} = \lambda^s \partial F / \partial \sigma_{ij}$) are used.

The consistency condition, $\dot{F} = 0$, can be expanded into

$$\frac{\partial F}{\partial p}\dot{p} + \frac{\partial F}{\partial q}\dot{q} + \frac{\partial F}{\partial p_i}\dot{p}_i + \frac{\partial F}{\partial M_i}\dot{M}_i = 0 \tag{12}$$

In numerical implementation, the last term involving M_i is a tad tedious and loses generality as it depends on the chosen idealization for the critical state function. The M_i term also varies in the π-plane as the Lode angle changes. It is both conceptual and practical that, because the last term on M_i in Equation (12) changes quite slowly compared with other terms, M_i is updated

only at the end of rather than during plastic correction. In other words, M_i is updated one step behind the corresponding calculation. In an explicit code like *FLAC3D*, this error is small because the steps are small. Equation (12) can thus be rewritten as

$$D^p \dot{p} + \dot{q} - M_i p \frac{\dot{p}_i}{p_i} = 0 \tag{13}$$

by noting that $\partial F / \partial p_i = -M_i p / p_i$. Combining Equations (8), (11), and (13), λ^s can be numerically solved. Once λ^s is known, the converged principal stress increments can be calculated (Jefferies et al. 2015).

The NorSand model is a stress-dependent model. Reasonable initial stress should be input the first time the NorSand model is assigned. The initial conditions include the initial stress, $\sigma_{ij,0}$, initial state, e_0 or ψ_0, and over-consolidation ratio, $OCR = p_i / p_{i,OCR=1}$, which is defined in this model as the ratio of the current p_i over the calculated $p_{i,OCR=1}$ so that the initial stress is on the "virtual" yield surface corresponding to $p_{i,OCR=1}$. The initial stress invariants, p_0, q_0 and the initial Lode's angle, θ_0, can be calculated from the initial stress. The determination of the initial image stress $p_{i,0}$ and the stress ratio at the image stress, $M_{i,0}$, needs an iteration procedure.

VERIFICATIONS

Verification checks that the model implementation is mathematically correct and coded correctly. Model verification requires the simulated results to be compared with closed-form solutions or with different codes developed independently. The NorSand model does not have any closed-form solution, so the results simulated at the element level by *FLAC3D* are compared with results from direct Euler integration coded in VBA using an Excel spreadsheet for triaxial compression and simple shear.

Table 1 Properties for the triaxial compression test

Property	C_a	C_b	M_{tc}	χ_{tc}	N	H_0	G_{ref}	m	υ	p_{ref}
Value	0.9	0.02	1.2	3.5	0.3	300	3e4	1	0.15	100

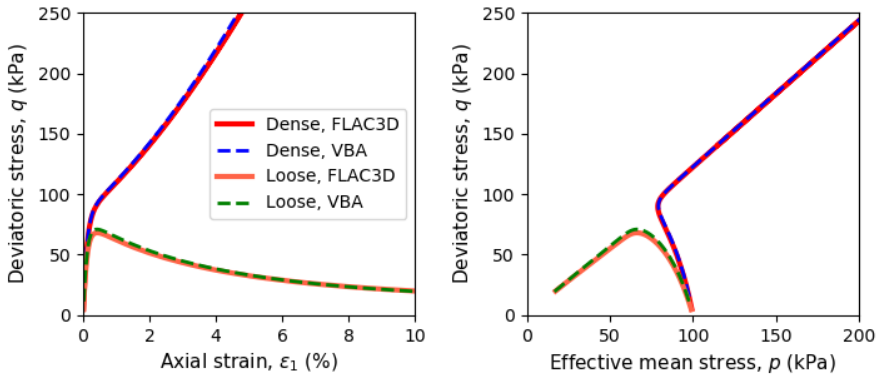

Figure 2: Results of simulation by FLAC3D and VBA for undrained triaxial compression tests for dense ($\psi_0 = -0.05$) and loose ($\psi_0 = 0.05$) sands.

Triaxial Compression: The NorSand model is used to simulate the triaxial consolidated

drained and undrained tests with the consolidated stress at 100 kPa. Two cases with different initial state parameters are considered to represent sands at dense ($\psi_0 = -0.05$) and loose ($\psi_0 = 0.05$) conditions, respectively. The material properties are listed in Table 1. Figure 2 plots the results of simulation by *FLAC3D* and VBA for drained triaxial compression tests for sands with $\psi_0 = -0.05$ and $\psi_0 = 0.05$, respectively. Very close results are found for both the shear hardening of dense sand and shear softening of loose sand. Figure 3 plots the results for undrained conditions. The dilative behavior for the dense sand and the contractive behavior for the loose sand are observed, with excellent agreement between *FLAC3D* and VBA.

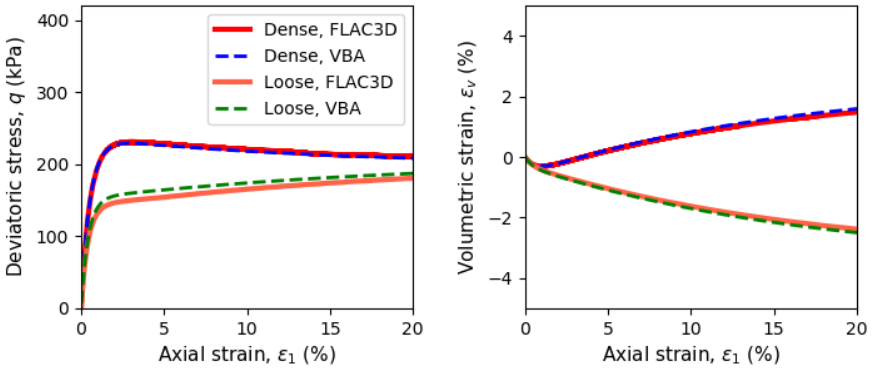

Figure 3: Results of simulation by FLAC3D and VBA for drained triaxial compression tests for dense ($\psi_0 = -0.05$) and loose ($\psi_0 = 0.05$) sands.

Simple Shear: The NorSand model is used to simulate the undrained simple shear tests with the initial effective vertical stress of 100 kPa and $K_0 = 0.5$. Again, two cases with different initial state parameters are considered: $\psi_0 = -0.05$ representing a loose sand and $\psi_0 = 0.05$ representing a dense sand. The material properties are the same as those listed in Table 1. Figure 4 plots the results of simulation by *FLAC3D* and VBA for undrained simple shear tests. Again, the agreement between *FLAC3D* and VBA is good.

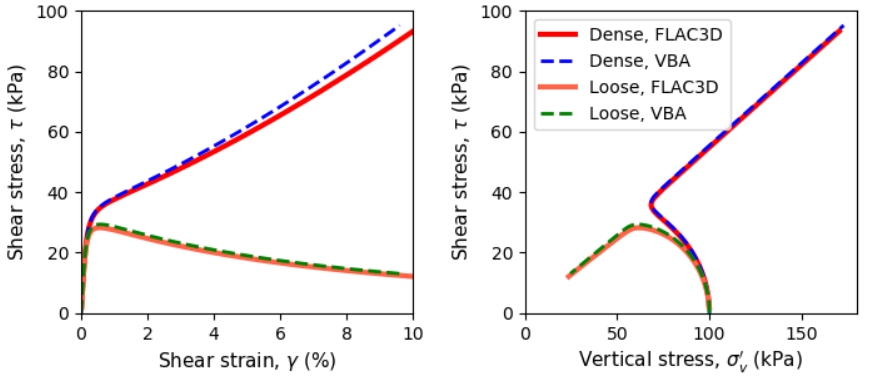

Figure 4: Results of simulation by FLAC3D and VBA for undrained simple shear tests for dense ($\psi_0 = -0.05$) and loose ($\psi_0 = 0.05$) sands.

Effect of Term T_s: This example is to test the optional cap softening term T_s by simulating the triaxial undrained tests with the initial isotropic stress at 395 kPa with and without the cap

softening. The material properties are listed in Table 2. Note that in these tests, the state-parameter-dependent hardening modulus ($H_y \neq 0$) and nonlinear stress dependent elastic shear modulus ($m \neq 1$) are adopted. The initial state parameter is $\psi_0 = 0.1$. Also, a slightly over-consolidated ratio (*OCR* = 1.1) is used, as that is often encountered with test data (presumed to be a consequence of common sample preparation protocols). Figure 5 plots the results of simulation by *FLAC3D* and VBA with and without the additional softening term by setting S = 0 or 1. It is observed that with the softening term, the rate of strength loss with strain is more rapid. The results between *FLAC3D* and VBA match very well.

Table 2 Properties for the test for effect of term T_s

Property	C_a	C_b	M_{tc}	χ_{tc}	N	H_0	H_y	G_{ref}	ν	p_{ref}	OCR
Value	1.2	0.06	1.47	3.2	0.5	75	400	20970	0.15	100	1.1

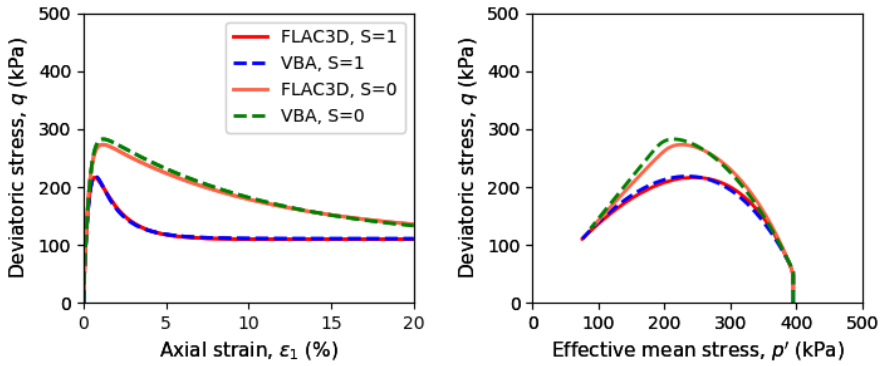

Figure 5: Results of simulation by FLAC3D and VBA for undrained triaxial compression tests for initial $\psi_0 = 0.1$, with ($S = 1$) or without ($S = 0$) the cap softening term T_S .

Table 3 Properties for the cyclic DSS test considering PSR effect

Property	C_a	C_b	C_c	S	M_{tc}	χ_{tc}	N	H_0	G_{ref}	ν	p_{ref}	Z
Value	0.95	6.2e-4	0.81	1	1.45	3.2	0.43	50	3.82e5	0.15	100	12

SIMULATION EXAMPLES

Undrained Cyclic DSS Loading: The NorSand model is used to simulate the undrained direct simple shear (DSS) test with the initial effective vertical stress of 100 kPa and $K_0 = 0.9$. The initial state parameter is $\psi_0 = -0.07$. The material properties are listed in Table 3. Note that in this test, the critical state line is defined by the three-parameter equation as in Equation (13) since $C_c \neq 0$. The simple shear cyclic magnitude is τ_{max} = kPa, which corresponds to *CSR* = 0.1, where CSR represents cyclic stress ratio. The effect of PSR is activated by setting a non-zero material parameter $Z = 12$. Figure 6 plots the results of simulated results by *FLAC3D* compared with the measured laboratory data on Fraser River Sand (Sriskandakumar 2004), including curves of shear stress vs. effective vertical stress, shear stress vs. shear strain, R_u (defined as $(p_0' - p')/p_0'$ vs. number of cycles, and R_u vs shear strain. As can be seen in the figure, the

overall cyclic behavior is satisfactory with only a limited number of material parameters.

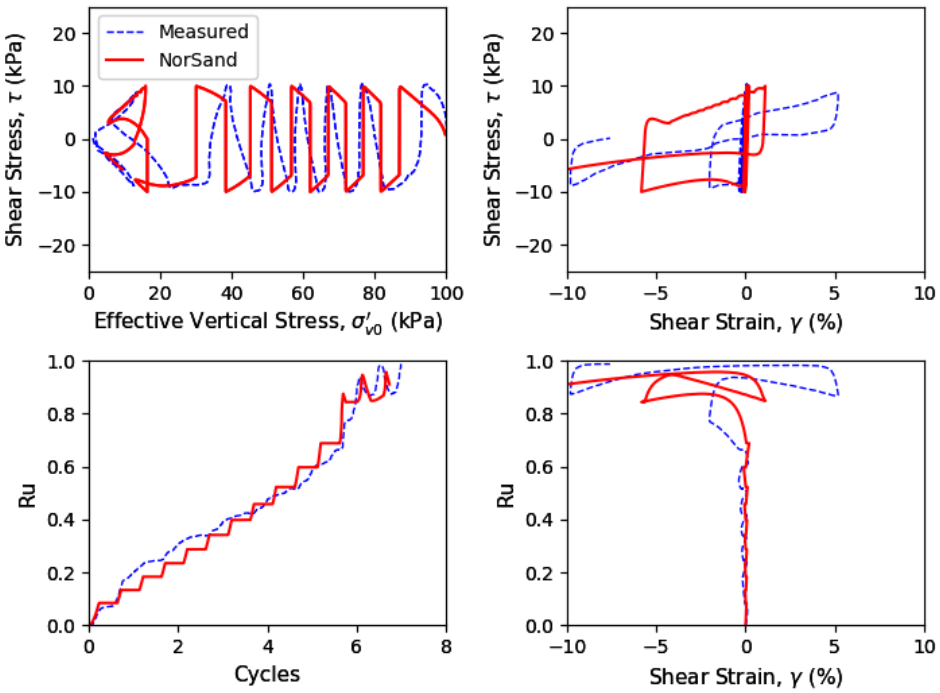

Figure 6: Simulated and measured DSS dynamic response considering PSR.

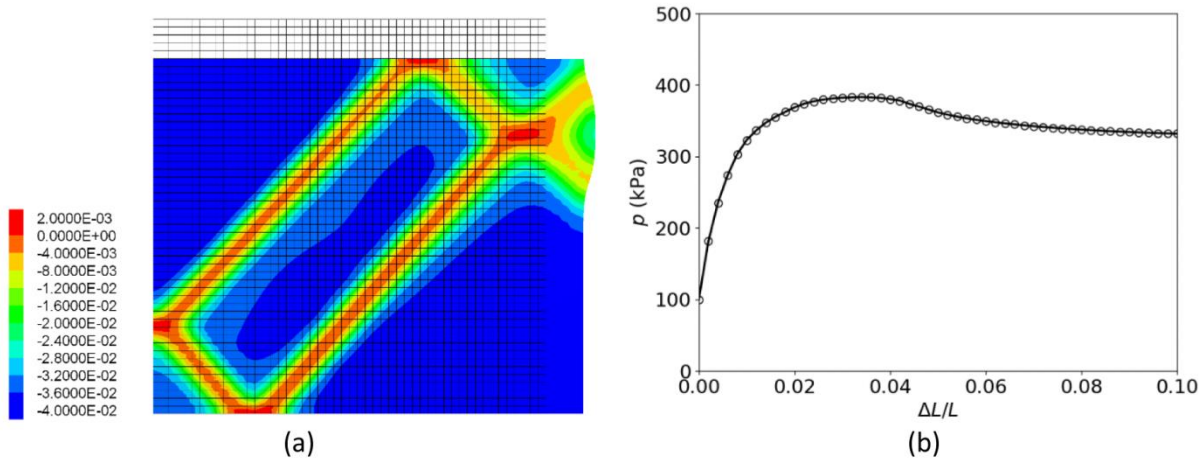

Figure 7: (a) Shear localization ("shear bands") in bi-axial loading illustrated by contours of state parameter; the undeformed and deformed grids are also plotted. (b) p vs. $\Delta L / L$.

Strain Localization: A relatively more complicated boundary-value problem simulation is illustrated in Figure 7. This is a plain-strain biaxial loading exercise with a grid with dimensions of 50×50 in the plane. The left side and the base are roller boundaries, the right side is subjected to a constant pressure of 100 kPa, and a fixed velocity boundary (with vertical strain rate of 1e-6) is applied at the top surface. The same material properties listed in Table 1 are used. The initial state parameter for all zones are $\psi_0 = -0.05$ and the stress in the model is isotopically initialized to 100 kPa. The loading continues until the vertical displacement ΔL is 10% of the model dimension L. Apparent strain localization (shear band) is observed due to the bifurcation of stress

paths. The state parameters in the "shear bands" become positive (dilative status) compared to initially negative values. The reactive pressure p at the model top surface versus $\Delta L/L$ is plotted in Figure 7, where the global softening is well captured. This example demonstrates the robustness of the implemented NorSand model.

SUMMARY

The updated NorSand model (as per Jefferies et al. 2015) incorporating the general 3D formulation with optional softening and principle stress rotation has been implemented in the widely used software package *FLAC3D*. The implementation is verified and validated by a wide range of tests with conditions including loose and dense soils, undrained and drained, triaxial compression and simple shear, and monotonic and cyclic loading. More complicated case studies are not included due to the length limit but hopefully will be presented elsewhere. This work provides a tool for practicing engineers to perform comprehensive analysis, including analysis of static liquefaction for important soil structures like tailing dams using a constitutive model with only a few familiar material properties.

REFERENCES

Been, K., and Jefferies, M. G. (1985). "A state parameter for sands." *Géotechnique*, 35(2), 99-112.

Drucker, D. C., Gibson, R. E., and Henkel, D. J. (1957). "Soil mechanics and work-hardening theories of plasticity." *Trans., ASCE* (122), 338-346.

Itasca (2019a), *FLAC — Fast Lagrangian Analysis of Continua*, user's manual, version 8.1, Itasca Consulting Group, Inc., Minneapolis, MN.

Itasca (2019b), *FLAC3D —Fast Lagrangian Analysis of Continua in 3 Dimensions*, user's manual, version 7.0. Itasca Consulting Group, Inc., Minneapolis, MN.

Jefferies, M. G. (1993). "Nor-Sand: a simple critical state model for sand." *Géotechnique*, 43(1), 91-103.

Jefferies, M. G., and Shuttle, D. A. (2002). "Dilatancy in general Cambridge-type models." *Géotechnique*, 52(9), 625-638.

Jefferies, M. G., and Shuttle, D. A. (2005). "NorSand: features, calibration and use." In *Soil Constitutive models: evaluation, selection, and calibration*. 204-236.

Jefferies, M. G., and Shuttle, D. A. (2011). "On the operating critical friction ratio in general stress states." *Géotechnique*, 61(8), 709-713.

Jefferies, M., Shuttle, D., and Been, K. (2015). "Principal stress rotation as cause of cyclic mobility." *Geotechnical Research*, 2(2), 66-96.

Jefferies, M., and Been, K. (2016). *Soil liquefaction, a critical state approach* (second edition). Boca Raton, London, New York: CRC Press.

Morgenstern, N. (chair), Vick, S., Viotti, C., and Watts, B. (2016). *Fundão tailings dam review panel report on the immediate causes of the failure of the Fundão dam*. Samarco S.A., Vale S.A.

Morgenstern, N. R. (chair), Jefferies, M., Van Zyl, D., and Wates, J. (2019). *Report on NTSF embankment failure*. Ashurst, Australia.

Nova, R. (1982). "A constitutive model for soil under monotonic and cyclic loading." In *Soil Mechanics: Transient and Cyclic Loads*, G. N. Pande, and O. C. Zienkiewicz, eds. Chichester: Wiley.

Sriskandakumar, S. (2004). “Cyclic loading response of Fraser sand for validation of numerical models simulating centrifuge tests.” Master's thesis, Department of Civil Engineering. The University of British Columbia.